Longitudinal magnetic fluctuations in Langevin spin dynamics

Pui-Wai Ma[*] and S. L. Dudarev[†]

EURATOM/CCFE Fusion Association, Culham Centre for Fusion Energy, Abingdon, Oxfordshire OX14 3DB, United Kingdom
(Received 30 April 2012; revised manuscript received 6 July 2012; published 13 August 2012)

We develop a generalized Langevin spin dynamics (GLSD) algorithm where both the longitudinal and transverse (rotational) degrees of freedom of atomic magnetic moments are treated as dynamic variables. This removes the fundamental limitation associated with the use of stochastic Landau-Lifshitz (sLL) equations, in which the magnitude of magnetic moments is assumed constant. A generalized Langevin spin equation of motion is shown to be equivalent to the sLL equation if the dynamics of an atomic moment vector is constrained to the surface of a sphere. A fluctuation-dissipation relation for GLSD and an expression for the dynamic spin temperature are derived using the Fokker-Planck equation. Numerical simulations, performed using ferromagnetic iron as an example, illustrate the fundamental difference between the two- and three-dimensional dynamic evolution of interacting moments, where the three-dimensional GLSD includes the treatment of both transverse and longitudinal magnetic excitations.

I. INTRODUCTION

Langevin spin dynamics (SD) treats thermal fluctuations of a single spin, or thermal excitations of an interacting spin ensemble, by introducing stochastic and dissipation terms in the spin equations of motion.[1] These two terms, steering a spin system towards thermal equilibrium, are related through the fluctuation-dissipation theorem.[2–4] Langevin SD is a versatile technique for simulating relaxation and equilibration processes in magnetic materials at finite temperatures.[5–17] For a variety of applications, Langevin SD is equivalent to the dynamics described by stochastic Landau-Lifshitz (sLL) or stochastic Landau-Lifshitz-Gilbert (sLLG) equations.[1,5–17]

The sLL equation has the form:

$$\frac{d\mathbf{S}}{dt} = \frac{1}{\hbar}[\mathbf{S} \times (\mathbf{H} + \mathbf{h}) - \gamma_s \mathbf{S} \times (\mathbf{S} \times \mathbf{H})], \qquad (1)$$

where $\mathbf{S} = -\mathbf{M}/g\mu_B$ is the spin vector of an atom, $\mathbf{M}$ is its magnetic moment, $\mathbf{H}$ is the effective field acting on an atomic spin, $\mathbf{h}$ is a fluctuating field, and γ_s is a damping parameter. Equation (1) conserves the magnitude of the spin vector $\mathbf{S}$. The same argument applies to the sLLG equation.

According to Eq. (1), a spin vector $\mathbf{S}(t)$ evolves dynamically, at each moment of time remaining on a two-dimensional surface of a sphere. The magnitude of the spin vector does not fluctuate, despite the fact that there is a fluctuating term in the right-hand side of Eq. (1). The lack of longitudinal fluctuations (LFs) is a fundamental drawback of Langevin SD. LFs of magnetic moments are closely linked to the itinerant nature of electron magnetism, where electron-electron exchange interaction is responsible for the formation of local atomic magnetic moments. LFs have a significant effect on the high-temperature properties of a magnetic alloy such as its free energy[18,19] and specific heat.[20,21] LFs of magnetic moments also influence finite-temperature properties and dynamics of defects and dislocations. For example, density functional calculations show substantial variations of magnitudes of magnetic moments in the strongly distorted core regions of defect structures, at surfaces and interfaces.[22–27] Finite-temperature properties of defects play an important part in

determining high-temperature deformation modes of structural materials, such as iron alloys and steels.[18,26,28–30]

There are several computational methods that include the treatment of longitudinal and transverse magnetic degrees of freedom at finite temperatures. The majority of them are based on equilibrium finite-temperature *ab initio* calculations, for example dynamic mean field theory,[31] coherent potential approximation,[32] spin-fluctuation theory,[33,34] and quantum Monte Carlo simulations.[19] On a semiclassical level, the *ab initio* calculated electronic structure and interactions between magnetic moments are used as input for Monte Carlo[20,35] or spin dynamics[14–17] simulations.

Many of the above methods do not attempt to follow the real-time dynamics of the magnetic system. A notable exception is an approach that links classical spin dynamics with density functional theory.[14–17] In this approach, the effective intersite interactions between magnetic moments and the magnitudes of moments are calculated using density functional theory. Subsequently, evolution of the transverse (rotational) degrees of freedom of the spin vectors is followed using a system of coupled sLL equations.[14–17] Such an approach is still fairly computationally demanding, and simulations can only be performed for relatively small systems involving up to a thousand magnetic moments.

In this paper, we develop a method that makes it possible to include LFs in a semi-classical dynamics of evolution of interacting magnetic moments. The method is based on the generalization of Langevin SD to a fully three-dimensional stochastic dynamics of moments. In the generalized Langevin SD, both the longitudinal and rotational degrees of freedom of atomic spin vectors are treated on equal footing. This removes a fundamental limitation associated with the lack of longitudinal fluctuations in the sLL(G) equations, but retains the capacity of the method to simulate a very large system of interacting spins.

The paper is organized as follows. We first revisit the derivation of spin dynamics equations starting from a quantum-mechanical Hamiltonian and show that the method corresponds to the mean-field treatment of the effective field acting on the spins. Then, we derive the generalized Langevin spin dynamics (GLSD) equations of motion and prove that

these equations are equivalent to the sLL equations if the motion of a spin vector is constrained to a two-dimensional surface of a sphere. A Fokker-Planck equation is then used for establishing a fluctuation-dissipation relation. Numerical simulations, carried out using ferromagnetic iron as a model example, illustrate and compare predictions derived from two- and three-dimensional dynamics of magnetic moments.

II. THEORY

A. Mean-field approximation

For a closed system described by a spin Hamiltonian $\hat{\mathcal{H}}$, cf. Refs. 14 and 36, an equation of motion for a spin operator can be derived using the Poisson brackets commutator, viz.,

$$\frac{d\hat{\mathbf{S}}}{dt} = \frac{i}{\hbar}[\hat{\mathcal{H}}, \hat{\mathbf{S}}]. \qquad (2)$$

On the other hand, classical equations of motion for a spin vector are usually given in the form[1,5,6,10–12,17]

$$\frac{d\mathbf{S}}{dt} = \frac{1}{\hbar}(\mathbf{S} \times \mathbf{H}), \qquad (3)$$

where

$$\mathbf{H} = -\frac{\partial \mathcal{H}}{\partial \mathbf{S}} \qquad (4)$$

is the effective vector field acting on spin $\mathbf{S}$. Equation (3) conserves the total energy for a closed system, and hence satisfies a fundamental condition of Hamiltonian dynamics. Still, the range of validity of this equation remains not very well defined. To clarify the meaning of Eq. (4), we undertake a brief derivation showing that Eqs. (2) and (3) are closely related, and that Eq. (3) in fact represents the mean-field limit of Eq. (2), cf. Ref. 37.

Assuming an arbitrary quantum-mechanical Hamiltonian, expressed in terms of spin operators, we write it in the form of a Taylor series

$$\hat{\mathcal{H}} = \sum_{n=0}^{\infty} \mathbf{a}_n \hat{\mathbf{S}}^n, \qquad (5)$$

where $\hat{\mathbf{S}} = (\hat{S}_x, \hat{S}_y, \hat{S}_z)$ is a spin operator and $\mathbf{a}_n$ is a Taylor expansion coefficient. A similar representation can be constructed for a system described by an arbitrary set of spin operators in which $\mathbf{a}_n$ is a multidimensional tensor with indexes referring to individual spins.

We now write each term in Eq. (5) in the form

$$\hat{\mathbf{S}}^n = (\langle\hat{\mathbf{S}}\rangle + \hat{\mathbf{S}} - \langle\hat{\mathbf{S}}\rangle)^n, \qquad (6)$$

where $\langle\hat{\mathbf{S}}\rangle$ is the expectation value of $\hat{\mathbf{S}}$. Defining

$$\delta\hat{\mathbf{S}} = \hat{\mathbf{S}} - \langle\hat{\mathbf{S}}\rangle, \qquad (7)$$

we transform Eq. (6) as

$$\hat{\mathbf{S}}^n = \langle\hat{\mathbf{S}}\rangle^n + n\langle\hat{\mathbf{S}}\rangle^{n-1}\delta\hat{\mathbf{S}} + \cdots. \qquad (8)$$

Substituting this into the Taylor series for the spin Hamiltonian, Eq. (5), we arrive at

$$\hat{\mathcal{H}} = \sum_{n=0}^{\infty} \mathbf{a}_n \langle\hat{\mathbf{S}}\rangle^n + \sum_{n=1}^{\infty} \mathbf{a}_n n \langle\hat{\mathbf{S}}\rangle^{n-1}\delta\hat{\mathbf{S}} + \cdots. \qquad (9)$$

Since the expectation value of operator $\langle\hat{\mathbf{S}}\rangle$ is the spin vector $\mathbf{S}$ itself, we see that the first term in Eq. (9) represents the Hamiltonian *function*, $\mathcal{H}$, which is defined as the Hamiltonian, Eq. (5), in which all the spin operators are replaced by their expectation values. The Hamiltonian function commutes with any spin operator and hence gives no contribution to the commutator in the right-hand side of the Poisson bracket, Eq. (2). The first nonvanishing contribution to equations of motion comes from the second sum in the right-hand side of Eq. (9), which has the form

$$\sum_{n=1}^{\infty} \mathbf{a}_n n \mathbf{S}^{n-1}\delta\hat{\mathbf{S}} = \frac{\partial\mathcal{H}}{\partial\mathbf{S}} \cdot \delta\hat{\mathbf{S}} = -\mathbf{H} \cdot (\hat{\mathbf{S}} - \langle\hat{\mathbf{S}}\rangle). \qquad (10)$$

Here, vector $\mathbf{H} = -\partial\mathcal{H}/\partial\mathbf{S}$ also commutes with $\hat{\mathbf{S}}$. Using the commutation relations for the spin operators, we arrive at the equation of motion for the spin operators

$$\frac{d\hat{\mathbf{S}}}{dt} = \frac{1}{\hbar}\left[\hat{\mathbf{S}} \times \left(-\frac{\partial\mathcal{H}}{\partial\mathbf{S}}\right)\right], \qquad (11)$$

which, being linear in spin operators, has the same form as the classical equation (3) for the spin vector. Our derivation is valid for any spin Hamiltonian $\hat{\mathcal{H}}$, and hence the spin equations of motion investigated below are valid for any interacting spin system, where the effective field acting on each spin is treated in the mean-field approximation.

B. Langevin equations of motion

In the semiclassical limit, taking the expectation values of both sides in Eq. (11), we write the equation of motion for a spin vector $\mathbf{S}_i(t)$ as

$$\frac{d\mathbf{S}_i}{dt} = \frac{1}{\hbar}(\mathbf{S}_i \times \mathbf{H}_i), \qquad (12)$$

where $\mathbf{H}_i = -\partial\mathcal{H}/\partial\mathbf{S}_i$, and $\mathbf{S}_i$ as well as $\mathbf{H}_i$ are three-dimensional vectors. As we noted in the Introduction, the corresponding *Langevin* spin equations of motion are commonly taken in the form of sLL equations, namely,

$$\frac{d\mathbf{S}_i}{dt} = \frac{1}{\hbar}[\mathbf{S}_i \times (\mathbf{H}_i + \mathbf{h}_i) - \gamma_s \mathbf{S}_i \times (\mathbf{S}_i \times \mathbf{H}_i)]. \qquad (13)$$

The fluctuating field $\mathbf{h}_i$ entering this equation is related to the damping parameter γ_s through the fluctuating-dissipation relation,[1–4,7,9] namely, $\langle\mathbf{h}_i(t)\rangle = 0$, $\langle h_{i\alpha}(t)h_{j\beta}(t')\rangle = \mu_s \delta_{ij}\delta_{\alpha\beta}\delta(t - t')$ and $\mu_s = 2\gamma_s\hbar k_B T$. Here, subscripts α and β denote the Cartesian components of a vector. We note that colored, i.e., non-δ-correlated, noise has also been considered within the framework of the sLL equation.[38,39]

Comparing the sLL equation with the Langevin equation of motion for atoms,[2–4] we note that they look fairly dissimilar. The conventional forms of the Langevin equations of motion for interacting atoms are

$$\frac{d\mathbf{p}_i}{dt} = -\frac{\partial U}{\partial\mathbf{R}_i} - \gamma_l \frac{\mathbf{p}_i}{m} + \mathbf{f}_i, \qquad (14)$$

$$\frac{d\mathbf{R}_i}{dt} = \frac{\mathbf{p}_i}{m}, \qquad (15)$$

where $U = U(\{\mathbf{R}_i\})$ is the potential energy of interaction between the atoms, $\mathbf{R}_i$ is the position of atom i, $\mathbf{p}_i$ is its momentum, $\mathbf{f}_i$ is a δ-correlated fluctuating force, and γ_l is a damping

parameter. The Hamiltonian function for interacting atoms is

$$\mathcal{H} = \sum_i \frac{\mathbf{p}_i^2}{2m} + U(\{\mathbf{R}_i\}). \tag{16}$$

To establish a connection between the Langevin treatment of motion of atoms and Langevin equations for the spins, we note that the dissipation term in Eq. (14) can be expressed in terms of the partial derivative of the Hamiltonian function with respect to the momentum of an atom as

$$-\gamma_l \frac{\mathbf{p}_i}{m} \rightarrow -\gamma_l \frac{\partial \mathcal{H}}{\partial \mathbf{p}_i}. \tag{17}$$

Dissipative terms proportional to the partial derivatives of the Hamiltonian function with respect to particle coordinates $\partial \mathcal{H}/\partial \mathbf{R}_i$ can also be included in Eq. (15), see Refs. 40 and 41.

Applying the same principle, we write the Langevin spin equations of motion as

$$\frac{d\mathbf{S}_i}{dt} = \frac{1}{\hbar} \left[\mathbf{S}_i \times \left(-\frac{\partial \mathcal{H}}{\partial \mathbf{S}_i} \right) \right] - \gamma_s' \frac{\partial \mathcal{H}}{\partial \mathbf{S}_i} + \boldsymbol{\xi}_i \tag{18}$$

$$= \frac{1}{\hbar} (\mathbf{S}_i \times \mathbf{H}_i) + \gamma_s' \mathbf{H}_i + \boldsymbol{\xi}_i \tag{19}$$

where $\boldsymbol{\xi}_i$ is a δ-correlated fluctuating "force" acting on spin i. In what follows, we assume that this force satisfies the usual conditions $\langle \boldsymbol{\xi}_i(t) \rangle = 0$ and $\langle \xi_{i\alpha}(t)\xi_{j\beta}(t') \rangle = \mu_s' \delta_{ij}\delta_{\alpha\beta}\delta(t - t')$. Equations (18) and (19) form the fundamental set of equations for GLSD. The key difference between Eq. (18) and the sLL equation (13) is that Eq. (18) no longer imposes any constraint on the magnitude of atomic spin, and in this way, it introduces longitudinal fluctuations of the spin vector.

It is natural to pose a question about the relationship between Eqs. (13) and (18). It is a simple matter to prove that Eq. (13) is nothing but a projection of Eq. (18) onto the surface of a sphere. To show this, we subtract longitudinal components from the vector terms describing dissipation and fluctuations or, in other words, apply the following transformation to Eq. (19):

$$\mathbf{H}_i \rightarrow \mathbf{H}_i - \mathbf{e}_i(\mathbf{e}_i \cdot \mathbf{H}_i), \tag{20}$$

$$\boldsymbol{\xi}_i \rightarrow \boldsymbol{\xi}_i - \mathbf{e}_i(\mathbf{e}_i \cdot \boldsymbol{\xi}_i), \tag{21}$$

where $\mathbf{e}_i = \mathbf{S}_i/S_i$ is a unit vector in the longitudinal direction of an atomic spin. Using vector algebra, we now transform the dissipation term as

$$\mathbf{H}_i - \mathbf{e}_i(\mathbf{e}_i \cdot \mathbf{H}_i) = -\mathbf{e}_i \times (\mathbf{e}_i \times \mathbf{H}_i). \tag{22}$$

The vector structure of the right-hand side of this equation is identical to that of the last term in the right-hand side of Eq. (13), hence proving the equivalence of Eqs. (13) and (19).

To show the equivalence between the fluctuation term entering Eq. (13) and the projection (21) of random force $\boldsymbol{\xi}(t)$ into a sphere, we note that achieving this amounts to demonstrating that both random processes have the same statistical properties. To prove this, let us introduce random vector processes

$$\mathbf{u}_i = \boldsymbol{\xi}_i - \mathbf{e}_i(\mathbf{e}_i \cdot \boldsymbol{\xi}_i), \tag{23}$$

$$\mathbf{v}_i = \mathbf{e}_i \times \boldsymbol{\xi}_i, \tag{24}$$

where Eq. (23) is just a projection of $\boldsymbol{\xi}(t)$ onto the surface of a sphere, and Eq. (24) has the same vector structure as the

random field term in Eq. (13). Evaluating statistical average values for both quantities, we find that

$$\langle \mathbf{u}_i(t) \rangle = \langle \mathbf{v}_i(t) \rangle = 0, \tag{25}$$

$$\langle u_{i\alpha}(t)u_{j\beta}(t') \rangle = \delta_{ij}(\delta_{\alpha\beta} - \langle e_{i\alpha}e_{i\beta} \rangle)\delta(t - t')$$
$$= \langle v_{i\alpha}(t)v_{j\beta}(t') \rangle. \tag{26}$$

Since the statistical properties of random vector process $\mathbf{u}_i(t)$ are the same as the statistical properties of random vector process $\mathbf{v}_i(t)$, in the Langevin spin equations we can replace $\boldsymbol{\xi}_i - \mathbf{e}_i(\mathbf{e}_i \cdot \boldsymbol{\xi}_i)$ with $\mathbf{e}_i \times \boldsymbol{\xi}_i$, and vice versa.

Therefore Eq. (18) or (19) can be transformed into Eq. (13) *exactly* if we constrain the dynamics of the spin vector to the surface of a sphere of radius S_i. Equations, relating the random force term entering Eqs. (18) and (19), the random field term in Eq. (13), and damping parameters γ_s' and γ_s, have the form

$$\boldsymbol{\xi}_i = S_i \mathbf{h}_i/\hbar, \tag{27}$$

$$\gamma_s' = S_i^2 \gamma_s / \hbar. \tag{28}$$

It can be readily verified that if $\mu_s = 2\gamma_s \hbar k_B T$, then the fluctuation-dissipation relation for Eq. (18) reads $\mu_s' = 2\gamma_s' k_B T$. This relation can also be proven using the Fokker-Planck equation, as discussed below.

Concluding this section, we note that the invariant, with respect to the choice of a system of coordinates, structure of Eq. (18) offers a new insight into the nature of relaxation of transverse and longitudinal magnetic degrees of freedom. The fact that by adopting a simple functional form for the fluctuation and dissipation terms in Eqs. (18) and (19), we arrive at a formalism equivalent to the sLL equation (13) shows that it is the *same* value of damping parameter γ_s' that describes relaxation of all the degrees of freedom of magnetic moments. The fact that it is the same damping parameter γ_s' that describes relaxation of both transverse and longitudinal degrees of freedom is in effect a corollary of the covariant structure of Eqs. (18) and (19).

C. The Fokker-Planck equation

To derive a relation between the fluctuation and dissipation terms in Eqs. (18) and (19), we map Eq. (18) onto the Fokker-Planck equation[42,43]:

$$\frac{\partial W}{\partial t} = -\sum_{i,\alpha} \frac{\partial}{\partial S_{i\alpha}}(A_{i\alpha}W) + \frac{1}{2}\sum_{i,j,\alpha,\beta} \frac{\partial^2}{\partial S_{i\alpha}\partial S_{j\beta}}(B_{i\alpha j\beta}W), \tag{29}$$

where $A_{i\alpha} = \lim_{\Delta t \to 0} \frac{1}{\Delta t}\langle S_{i\alpha} \rangle$ is the drift coefficient and $B_{i\alpha j\beta} = \lim_{\Delta t \to 0} \frac{1}{\Delta t}\langle S_{i\alpha}S_{j\beta} \rangle$ is the diffusion coefficient.

The drift and diffusion coefficients for the coordinates and momenta have the form[42,43]

$$\mathbf{A}_i = -\frac{1}{\hbar}\left(\mathbf{S}_i \times \frac{\partial \mathcal{H}}{\partial \mathbf{S}_i} \right) - \gamma_s' \frac{\partial \mathcal{H}}{\partial \mathbf{S}_i}, \tag{30}$$

$$B_{i\alpha j\beta} = \mu_s' \delta_{ij}\delta_{\alpha\beta}. \tag{31}$$

At equilibrium, where $\partial W/\partial t = 0$, the energy distribution approaches the Gibbs distribution $W = W_0 \exp(-\mathcal{H}/k_B T)$. Here, W_0 is a normalization constant. Substituting this

distribution into the Fokker-Planck equation, we find

$$\frac{\partial W}{\partial t} = \left(\gamma_s' - \frac{\mu_s'}{2k_BT}\right)$$
$$\times \left\{\sum_{i,\alpha}\left[\frac{\partial^2\mathcal{H}}{\partial S_{i\alpha}^2} - \frac{1}{k_BT}\left(\frac{\partial\mathcal{H}}{\partial S_{i\alpha}}\right)^2\right]\right\}W. \quad (32)$$

The condition of thermal equilibrium is satisfied if

$$\mu_s' = 2\gamma_s'k_BT, \quad (33)$$

which is the desired fluctuation-dissipation relation. Similarly, we find that

$$k_BT = \sum_{i,\alpha}\left(\frac{\partial\mathcal{H}}{\partial S_{i\alpha}}\right)^2 \Big/ \sum_{i,\alpha}\frac{\partial^2\mathcal{H}}{\partial S_{i\alpha}^2}. \quad (34)$$

This equation relates temperature at equilibrium to the state variables. In the numerical examples that we explore below, we use this expression to evaluate the instantaneous temperature of a system away from equilibrium. We also compare it with the expression for spin temperature that we derived in Ref. 8 for a dynamic spin system evolving without LFs.

III. APPLICATION

A. Heisenberg-Landau Hamiltonian

In transition metals, such as iron, local magnetic moments form due to intra-atomic exchange interaction between d electrons.[44–47] A simple model that describes both the intersite interactions and the on-site LFs of moments is the Heisenberg-Landau Hamiltonian:[18,33,35,48,49]

$$\mathcal{H} = \mathcal{H}_R + \mathcal{H}_L, \quad (35)$$

where

$$\mathcal{H}_R = -\frac{1}{2}\sum_{i,j}J_{ij}\mathbf{S}_i\cdot\mathbf{S}_j, \quad (36)$$

$$\mathcal{H}_L = \sum_i\left(AS_i^2 + BS_i^4 + CS_i^6\right). \quad (37)$$

The first term in Eq. (35) is the Heisenberg Hamiltonian that describes collective magnetic excitations, which in materials with relatively simple magnetic structure have the form of spin waves. The second term is the Landau expansion, which describes how energy varies as a function of the magnitude of spin. This term is intimately linked to the local band structure of the material. The time-reversal symmetry requirement results in the Landau expansion containing only even powers of S_i. We may treat Eqs. (36) and (37) as representing the rotational and longitudinal parts of the total Hamiltonian, bearing in mind that they are not entirely independent of each other.

The choice of the form of the Hamiltonian and its parameters does not affect the validity of Eq. (18), but it influences the results of simulations. In iron, d electrons are relatively strongly localized. The magnitude of atomic magnetic moments is almost independent of temperature.[20,50,51] Effects associated with interaction between the Heisenberg term and the Landau term are expected to be small. The concept of local band structure of iron remains valid even at fairly high temperature, and the Heisenberg-Landau Hamiltonian provides a good approximation for magnetic dynamics simulations. For treating other materials, such as nickel, where longitudinal fluctuations of moments are more pronounced, one could add extra terms to the Heisenberg Hamiltonian,[35,52,53] which describe variations of the local band structure due to changes in the atomic spin orientations. Higher-order terms[33] or angular dependence[54] can also be included in the Landau expansion.

We evaluate exchange parameters J_{ij} for bcc iron using a method developed by van Schilfgaarde et al.[55] in which the linear muffin-tin orbital (LMTO) method is combined with a Green's function (GF) technique. Calculations are performed using the generalized gradient approximation (GGA).[56] The lattice constant is set to be 2.8665 Å. We first assume that the range of J_{ij} includes the first and second nearest-neighbor atoms. The calculated J_{ij} for the first and second nearest neighbours, i.e., J_1 and J_2, are then rescaled according to the accumulated value of J_{ij} for an arbitrary interatomic distance and variable magnitude of magnetic moment M. We set $M = 2.2\mu_B$, and find $J_1 = 22.52$ meV and $J_2 = 17.99$ meV.

To find the coefficients of Landau expansion, we fit the energy versus magnetic moment curve following a method described in Refs. 46 and 47. First, we calculate the density of states (DOS), $D(E)$, for d electrons for a *nonmagnetic* state. Assuming that the Stoner model describes the ferromagnetic ground state, the Fermi levels for the spin up $\epsilon_{F\uparrow}$ and spin down states $\epsilon_{F\downarrow}$ are calculated assuming a fixed value of magnetic moment M and the number of d electrons N, that is,

$$M = \int_{-\infty}^{\epsilon_{F\uparrow}}D(E)dE - \int_{-\infty}^{\epsilon_{F\downarrow}}D(E)dE, \quad (38)$$

$$N = \int_{-\infty}^{\epsilon_{F\uparrow}}D(E)dE + \int_{-\infty}^{\epsilon_{F\downarrow}}D(E)dE. \quad (39)$$

The Stoner parameter can then be found as

$$I = (\epsilon_{F\uparrow} - \epsilon_{F\downarrow})/M. \quad (40)$$

Once we have evaluated the Stoner parameter I, the energy of the system as a function of M can be calculated as

$$E_{\text{tot}} = \int_{-\infty}^{\epsilon_{F\uparrow}}ED(E)dE + \int_{-\infty}^{\epsilon_{F\downarrow}}ED(E)dE - \frac{I}{4}M^2, \quad (41)$$

where the values of $\epsilon_{F\uparrow}$ and $\epsilon_{F\downarrow}$ for each M are calculated according to Eqs. (38) and (39). Then, we plot the energy E_{tot} as a function of M and fit it to the Landau expansion, retaining terms up to the sixth order in M, namely,

$$E_{\text{tot}}(M) \approx E_0 + aM^2 + bM^4 + cM^6. \quad (42)$$

Comparing Eqs. (35) and (42), and assuming that in the ground state all the spins are collinear, we find $A = a(g\mu_B)^2 + (\sum_m n_mJ_m)/2$, $B = b(g\mu_B)^4$, and $C = c(g\mu_B)^6$, where n_m is the number of spins in the mth nearest-neighbor shell.

Figure 1 shows the partial DOS for $3d$ electrons in iron. They were also calculated using the LMTO-GF approach. The PDOS for both magnetic and nonmagnetic states are shown. One can see that the Stoner model for iron approximates the variation of energy as a function of magnetic moment fairly well. The shape of PDOS for up and down spins in a ferromagnetic state resembles the PDOS for a nonmagnetic
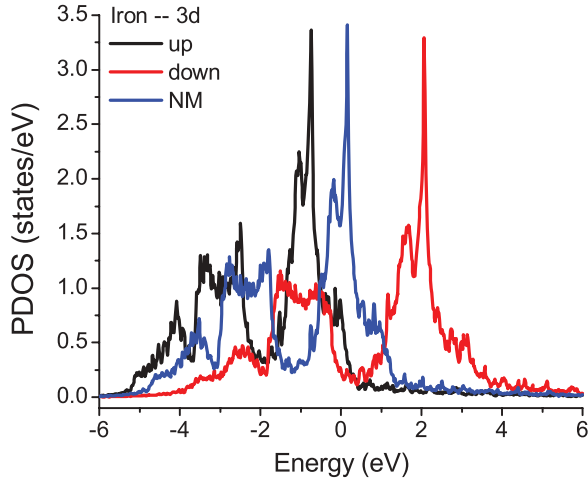
FIG. 1. (Color online) Partial densities of states (PDOS) for d electrons in bcc iron evaluated for magnetic and nonmagnetic (NM) states. The PDOS are calculated using the LMTO-GF method.[55] The PDOS for a nonmagnetic state is similar to the PDOS for spin up or down in the magnetic state. This confirms the rigid-band approximation underlying the Stoner model.

state, shifted up or down, in agreement with the assumptions underlying the Stoner model.

We extract the value of the Stoner parameter I from the nonmagnetic PDOS, which gives $I \approx 1.0$ eV. Energy as a function of M is calculated according to Eq. (41) and plotted in Fig. 2. We fit both the fourth- and sixth-order Landau expansions to the data. Although the fourth-order expansion already reproduces the shape of the $E_{tot}(M)$ curve fairly well, the sixth-order expansion provides a better fit to the curvature near the minimum energy point, which is important for the treatment of thermal fluctuations of M. From the fit, we find $A = -440.987$ meV, $B = 150.546$ meV, and $C = 50.6794$ meV.
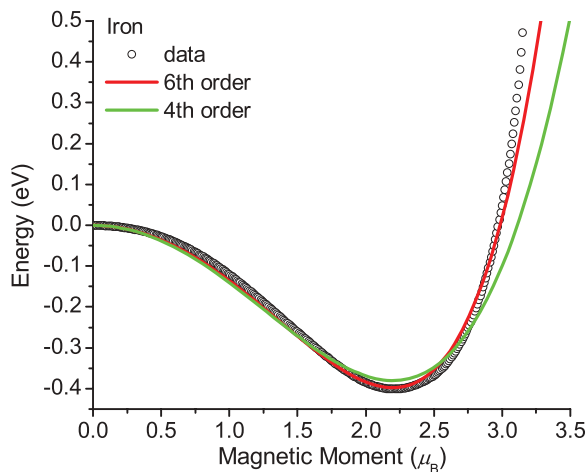

FIG. 2. (Color online) Energy as a function of M calculated according to Eq. (41). We fit both the fourth- and sixth-order Landau expansion coefficients to the data. Although the fourth-order expansion already reproduces the overall shape of the curve fairly well, the sixth-order expansion provides a much better fit to the curvature near the minimum energy point.

We note that the procedure described above is one of the many possible ways of extracting the exchange parameter[52,57–59] and coefficients of the Landau expansion[33,49,60] from the *ab initio* data. For example, the Landau expansion is not exact, although it approximates the electronic structure effects reasonably well. The profile of the DOS can also change due to the finite temperature effects. Here, we assume that the electronic structure at finite temperatures remains similar to that characterizing the ground state of the material. We also note that noncollinear fluctuations of magnetic moments associated with the Heisenberg term also modify the shape of the energy versus magnitude of magnetic moment curve. Below, we explore this effect using numerical simulations. A detailed discussion of this point can also be found in Ref. 48.

Examination of electronic band structure shows that the magnitude of magnetic moment is constrained from above, unless there are excitations with energy larger than the band gap. At the same time, the Landau expansion does not impose an upper limit on the magnitude of magnetic moment. Hence the Landau expansion overestimates the amount of phase space available for fluctuations of moments. However, it does not have a significant impact on the studies performed in this paper, since the range of temperatures of interest is very small in comparison with the electronic bandwidth.

B. Equilibrium data

Simulations were performed using cubic cells with 16 000 spins on bcc lattice. We performed simulations with and without LFs, using Eqs. (13) and (18), respectively. Thermal equilibrium energies per spin corresponding to various temperatures are plotted in Fig. 3. The fact that the reference energies at 0K differ is due to the Landau term, and is immaterial, whereas the variation of energy as a function of temperature is significant, since it is related to the slope of the curves, which represents the specific heat. By means of numerical differentiation we find the values of the specific heat $C = \partial \langle E \rangle / \partial T$ plotted in Fig. 4.
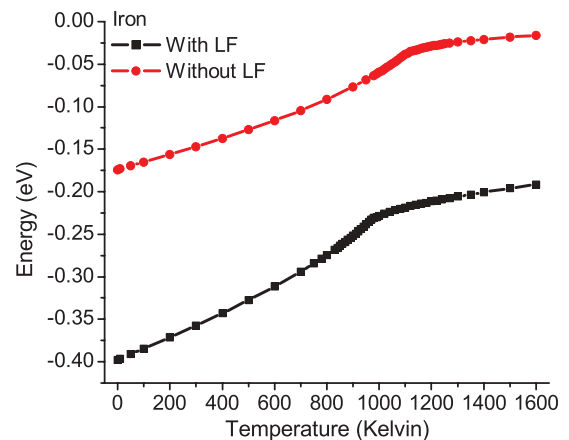

FIG. 3. (Color online) Thermal equilibrium energies per spin for bcc iron plotted as a function of temperature. Simulations were performed using Eq. (13) or (18), including or neglecting the effect of longitudinal fluctuations.
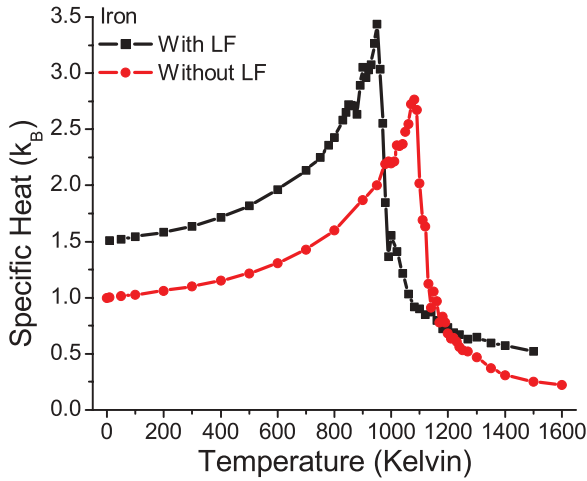
FIG. 4. (Color online) Specific heat of bcc iron vs temperature. This quantity is evaluated by performing numerical differentiation of data shown in Fig. 3. The peaks correspond to the Curie temperatures T_C (which differ depending on whether or not the effect of longitudinal magnetic fluctuations is taken into account).

Abrupt changes in the slope of the curves in Fig. 3 are responsible for the peaks shown in Fig. 4. They correspond to the Curie temperatures T_C, which are the temperatures at which the long-range magnetic order, and macroscopic magnetization, vanishes. Magnetization per atom versus temperature is plotted in Fig. 5. The calculated value of T_C for iron, with LFs included, is 950 K, whereas the same quantity calculated without taking LFs into account is 1050 K. For comparison, the experimental value of T_C is 1043 K.

Both calculated values for the Curie temperature are in reasonable agreement with observations, and simulations show that longitudinal fluctuations of magnetic moments reduce this temperature. This result differs from the earlier analysis by Ruban *et al.*[20] where it was found that the occurrence of LFs increases the T_C. It is possible that the increase of T_C noted in Ref. 20 may be due to the terms included for maintaining the global magnetization of the material. These terms bring the calculated value of T_C for nickel closer to observations.
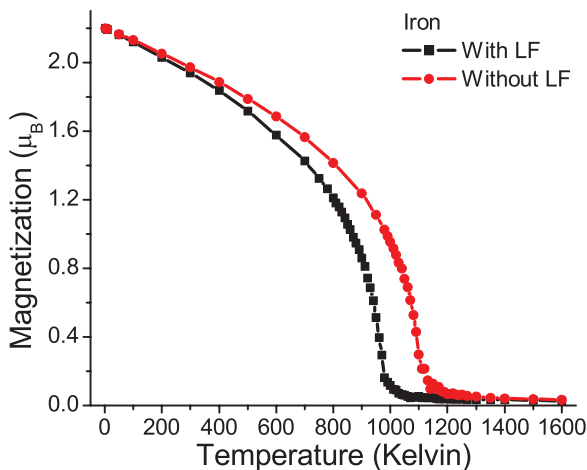

FIG. 5. (Color online) Magnetization of bcc iron vs temperature. Magnetization vanishes at the Curie temperature T_C.

The spin dynamics simulations discussed here do not include quantum fluctuation effects. Hence the specific heat does not vanish at $T = 0$ K. If LFs are taken into account in simulations, the specific heat at zero temperature approaches $1.5k_B$, compared to $1k_B$ in the limit with no LFs. At high temperatures, the specific heat of the spin system exhibiting LFs approaches $0.5k_B$, and does not vanish, as it does in a model where LFs are absent. The difference of $0.5k_B$ between the specific heat values found for the two cases is entirely due to the extra longitudinal degree of freedom included in the three-dimensional spin dynamics described by Eqs. (18) and (19). Indeed, a spin system exhibiting LFs is able to absorb energy at arbitrarily high temperatures. On the other hand, if the spins have only the rotational (transverse) degrees of freedom, they cannot absorb energy once the system reaches the maximum-entropy fully disordered high-temperature configuration. This finding agrees with the results by Lavrentiev *et al.*,[18,51] who performed classical equilibrium Monte Carlo simulations of high-temperature magnetic excitations in iron and iron-chromium alloys using the magnetic cluster expansion.

Figure 6 shows the average value and the standard deviation of the magnitude of magnetic moments $|\mathbf{M}_i|$ calculated taking into account LFs at various temperatures. The average moment decreases from $2.2\mu_B$ at 0 K to about $2.04\mu_B$ at T_C. This
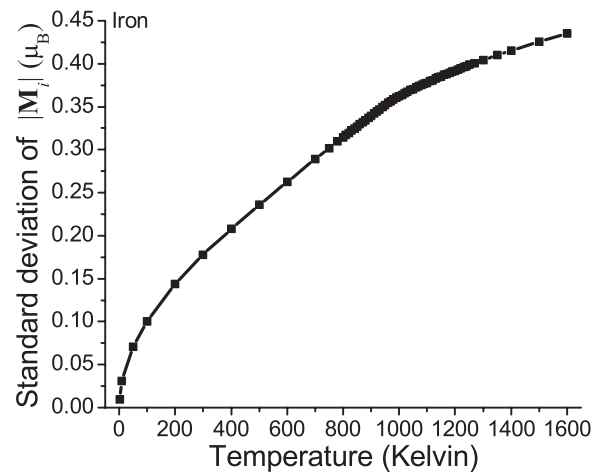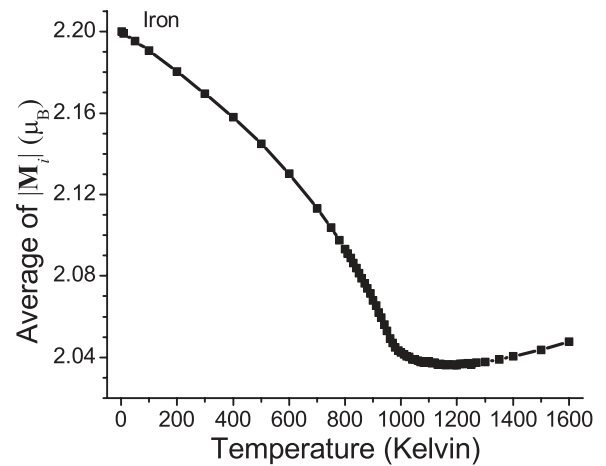

FIG. 6. The average value and the standard deviation of the magnitude of an atomic magnetic moment plotted as functions of temperature.
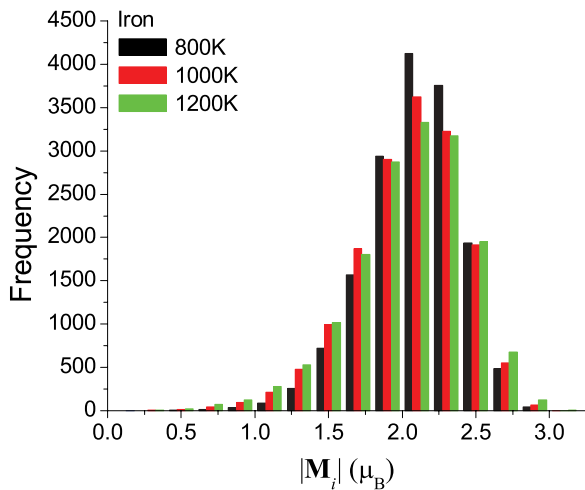
FIG. 7. (Color online) Histogram showing the distribution of the magnitude of magnetic moments at 800, 1000, and 1200 K computed for a simulation cell containing 16 000 spins.

can be interpreted as an anharmonic effect resulting from the asymmetry of the Landau energy well (see Fig. 2), combined with the perturbation resulting from the Heisenberg term. The standard deviation of the moment increases monotonically as a function of temperature. The fact that the atoms retain their magnetic moment above T_C is consistent with neutron scattering experiments,[61–65] which show that short-range magnetic order does not vanish above T_C. The increase of the average magnitude $|\mathbf{M}_i|$ of the moment beyond T_C is comparable with the earlier findings by Hasegawa *et al.*[50] and Lavrentiev *et al.*[51] and differs somewhat from the results by Ruban *et al.*[20] In Ref. 20, the authors discovered a slight ($0.1\mu_B$) overall reduction in the magnitude of the magnetic moment in the temperature range from T_C to 1500 K, whereas we find that the magnitude of the moment increases by approximately $0.01\mu_B$ over the same temperature interval. The difference is genuinely minor, and it illustrates the significance of using accurate values of the Landau expansion coefficients in Eq. (42). Figure 7 shows that the increase of the average value of $|\mathbf{M}_i|$ at high temperature is associated with the fact that more local moments have larger magnitude, with some moments having magnitudes in excess of $2.5\mu_B$. The distribution of moments is similar to the distribution found in Ref. 20.

C. Thermalization process

The advantage offered by spin dynamics simulations over equilibrium Monte Carlo simulations using the same Heisenberg-Landau Hamiltonian[21,51] is that instead of treating only the equilibrium magnetic properties of the material, we are now able to follow the dynamics of thermalization process at the microscopic level, including the investigation of dynamics of equilibration of the spin system and its response to thermal excitations. We simulate the time-dependent transient relaxation of large interacting spin systems to equilibrium starting from ferromagnetic ground states. All the simulations were performed assuming the value of the damping parameter $\gamma_s = 8 \times 10^{-3}$, which was found by fitting simulations to laser pulse induced demagnetization experimental data on iron thin
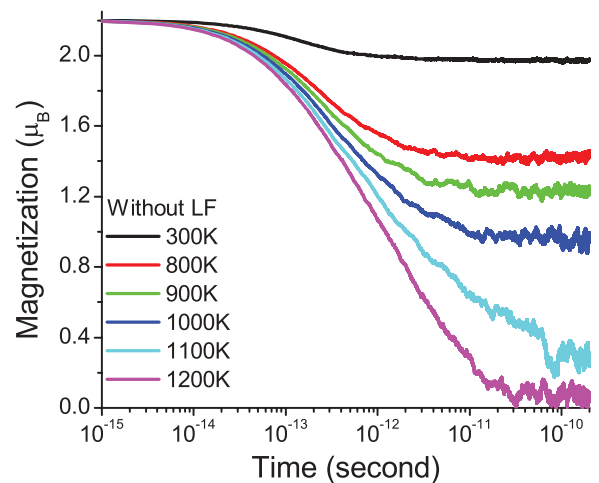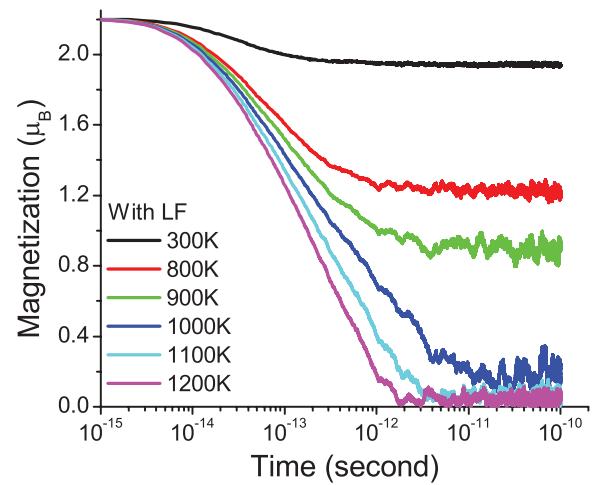

FIG. 8. (Color online) Total magnetization as a function of time simulated for a transient process of relaxation to thermal equilibrium. All the simulations were performed starting from ferromagnetic ground states.

films.[66,67] According to Eq. (28), this value of γ_s corresponds to $\gamma_s' = 5.88 \times 10^{13}$ eV^{-1}s^{-1}.

Figure 8 shows the evolution of magnetization as a function of time. Simulations show that at low temperatures, the characteristic thermalization timescale is not very sensitive to whether or not LFs are included in the model. However, as the temperature approaches T_C, LFs start playing a significant part, accelerating thermalization. This can be interpreted as a phase space effect where in the absence of LFs the dynamics of equilibration involves evolution of spin vectors constrained to a hypersurface in the spin space, where the instantaneous position of each spin is constrained to the surface of its own sphere. If LFs are present, the spin vectors are able to explore the entire three-dimensional spin space, and the system is able to attain equilibrium over a much shorter interval of time.

In dynamic spin simulations, we can monitor the *instantaneous temperature* of the system during the thermalization process. In Ref. 8, we derived an expression for dynamic spin temperature, which only applies if LFs are absent. In what follows, we refer to that temperature as the temperature for the rotational (transverse) degrees of freedom of atomic spins.
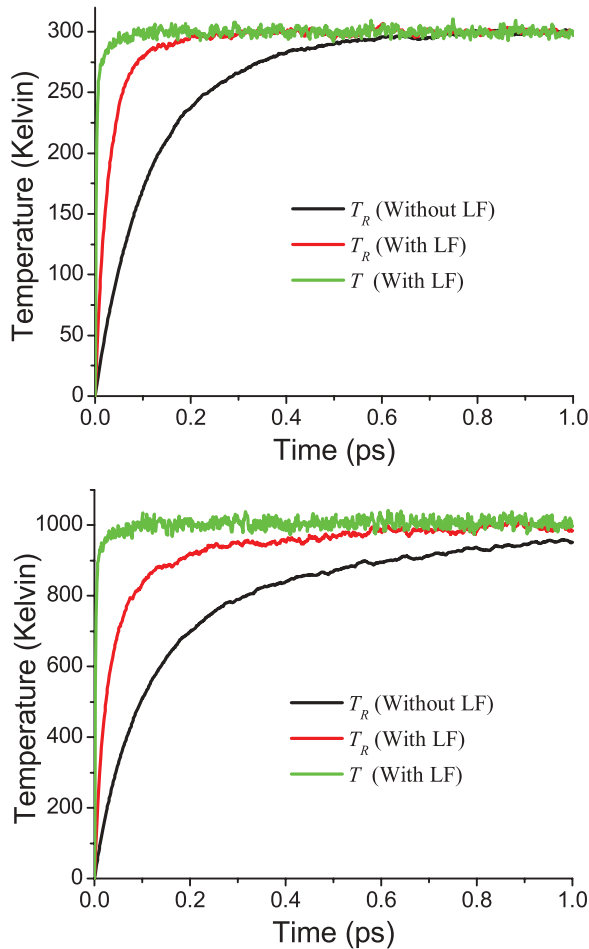
FIG. 9. (Color online) Temperatures evaluated using Eqs. (34) and (43) as functions of time during the thermalization process, with thermostats set at 300 K (upper) and 1000 K (lower).

The expression for the rotational temperature has the form[8]

$$T_R = \frac{\sum_i |\mathbf{S}_i \times \mathbf{H}_{Ri}|^2}{2k_B \sum_i \mathbf{S}_i \cdot \mathbf{H}_{Ri}}, \qquad (43)$$

where $\mathbf{H}_{Ri} = -\partial \mathcal{H}_R/\partial \mathbf{S}_i$. A more general expression for dynamic spin temperature, given by Eq. (34), also includes the effect of longitudinal fluctuations. Rigorously speaking, Eqs. (34) and (43) are only valid if a system is at perfect equilibrium. However, in dynamic simulations, we can still use those equations in order to monitor temperature as a function of time for transient nonequilibrium configurations, similarly to how temperature is monitored in conventional molecular dynamics simulations through the average squared velocity of atoms.

Figure 9 shows how temperatures evaluated using Eqs. (34) and (43) vary for cases where LFs were/were not included in the treatment of thermalization, with thermostats set at 300 and 1000 K. Similarly to the curve showing the transient variation of magnetization for a system interacting with a thermostat at 1000 K, relaxation of T_R in the case where LFs were not included in simulations occurs over a much longer period of time than in the case where LFs were included. Moreover, we see that temperature T defined by Eq. (34)

attains the equilibrium value much quicker than T_R in the case where LFs were included. This shows that the rate of absorption of energy through intersite spin-spin correlation is lower than the rate of absorption involving all the degrees of freedom of the system, confirming that on-site longitudinal fluctuations of moments play an important part in this process.

As a final remark, we note that GLSD can be readily incorporated into spin-lattice[7] or spin-lattice-electron dynamics[66] simulation frameworks, provided that fixed values of parameters J_{ij}, A, B, and C are replaced by functions of atomic positions $\{\mathbf{R}_i\}$. In the case of spin-lattice-electron dynamics, the electron-spin heat transfer coefficient G_{es} can be found by following a procedure similar to that described in Ref. 66. We differentiate Eq. (35) with respect to time, and evaluate ensemble average with the help of the Furutsu-Novikov theorem.[68–71] Assuming that the amplitude of fluctuations is solely determined by the temperature of an external thermostat T_e, meaning that $\mu_s' = 2k_B \gamma_s' T_e$, we arrive at

$$\frac{d\langle E \rangle}{dt} = k_B \gamma_s' \sum_{i,\alpha} \left\langle \frac{\partial^2 \mathcal{H}}{\partial S_{i\alpha}^2} \right\rangle (T_e - T). \qquad (44)$$

By comparing Eq. (44) with the heat transfer equation for electrons, including coupling to the spin subsystem, that is,

$$C_e \frac{dT_e}{dt} = G_{es}(T_s - T_e), \qquad (45)$$

we find that $G_{es} = k_B \gamma_s' \sum_{i,\alpha} \langle \partial^2 \mathcal{H}/\partial S_{i\alpha}^2 \rangle$. This shows that we can safely replace the sLL equation used in the spin-lattice-electron dynamics simulation method by the generalized Langevin spin equation of motion.

IV. CONCLUSIONS

We develop and prove the validity of a new form of Langevin spin dynamics. We call it generalized Langevin spin dynamics as it includes the treatment of evolution of both transverse and longitudinal magnetic degrees of freedom of atoms. The method does not impose a constraint on the magnitude of atomic spins (or, equivalently, the atomic magnetic moment), unlike the conventional Langevin spin dynamics, based on stochastic Landau-Lifshitz equations, which constrains the motion of atomic spins to two-dimensional spherical surfaces. Longitudinal degrees of freedom of moments can now be treated on the same footing as their transverse (rotational) degrees of freedom. The generalized Langevin spin equations of motion transform into the conventional equations of spin dynamics if the longitudinal degrees of freedom are projected out of the evolution equations. Simulations, illustrating applications of the method, use iron as an example, where transverse and longitudinal degrees of freedom are described by a suitably parameterized Heisenberg-Landau Hamiltonian. Using the new approach, we evaluate the equilibrium value of energy, specific heat and the distributions of magnitudes of magnetic moments, and explore the dynamics of spin thermalization, which all appear compatible with the known simulations and experimental observations.

*leo.ma@ccfe.ac.uk

†sergei.dudarev@ccfe.ac.uk

[1] W. F. Brown, Jr., Phys. Rev. **130**, 1677 (1963).

[2] S. Chandrasekhar, Rev. Mod. Phys. **15**, 1 (1943).

[3] R. Kubo, Rep. Prog. Phys. **29**, 255 (1966).

[4] W. Coffey, Yu. P. Kalmykov, and J. T. Waldron, *The Langevin Equation*, 2nd ed. (World Scientific, Singapore, 2004).

[5] J. L. García-Palacios and F. J. Lázaro, Phys. Rev. B **58**, 14937 (1998).

[6] O. Chubykalo, R. Smirnov-Rueda, J. M. Gonzalez, M. A. Wongsam, R. W. Chantrell, and U. Nowak, J. Magn. Magn. Mater. **266**, 28 (2003).

[7] P.-W. Ma, C. H. Woo, and S. L. Dudarev, Phys. Rev. B **78**, 024434 (2008); also in *Electron Microscopy and Multiscale Modeling*, edited by A. S. Avilov *et al.*, AIP Conf. Proc. No. 999 (AIP, New York, 2008), p. 134.

[8] P.-W. Ma, S. L. Dudarev, A. A. Semenov, and C. H. Woo, Phys. Rev. E **82**, 031111 (2010).

[9] P.-W. Ma and S. L. Dudarev, Phys. Rev. B **83**, 134418 (2011).

[10] J. H. Mentink, M. V. Tretyakov, A. Fasolino, M. I. Katsnelson and Th. Rasing, J. Phys.: Condens. Matter **22**, 176001 (2010).

[11] B. Skubic, J. Hellsvik, L. Nordström, and O. Eriksson, J. Phys.: Condens. Matter **20**, 315203 (2008).

[12] I. Radu, K. Vahaplar, C. Stamm, T. Kachel, N. Pontius, H. A. Dürr, T. A. Ostler, J. Barker, R. F. L. Evans, R. W. Chantrell, A. Tsukamoto, A. Itoh, A. Kirilyuk, Th. Rasing, and A. V. Kimel, Nature (London) **472**, 205 (2011).

[13] D. P. Landau and K. Binder, *A Guide to Monte Carlo Simulations in Statistical Physics* (Cambridge University Press, Cambridge, 2005), pp. 389–393.

[14] V. P. Antropov, M. I. Katsnelson, B. N. Harmon, M. van Schilfgaarde, and D. Kusnezov, Phys. Rev. B **54**, 1019 (1996).

[15] V. P. Antropov, S. V. Tretyakov, and B. N. Harmon, J. Appl. Phys. **81**, 3961 (1997).

[16] V. Antropov, Phys. Rev. B **72**, 140406 (2005).

[17] M. Fähnle, R. Drautz, R. Singer, D. Steiauf, and D. V. Berkov, Comput. Mater. Sci. **32**, 118 (2005).

[18] M. Y. Lavrentiev, D. Nguyen-Mahn, and S. L. Dudarev, Phys. Rev. B **81**, 184202 (2010).

[19] F. Körmann, A. Dick, B. Grabowski, B. Hallstedt, T. Hickel, and J. Neugebauer, Phys. Rev. B **78**, 033102 (2008); **81**, 134425 (2010); F. Körmann, A. Dick, T. Hickel, and J. Neugebauer, *ibid.* **83**, 165114 (2011).

[20] A. V. Ruban, S. Khmelevskyi, P. Mohn, and B. Johansson, Phys. Rev. B **75**, 054402 (2007).

[21] M. Yu. Lavrentiev, S. L. Dudarev, and D. Nguyen-Manh, J. Appl. Phys. **109**, 07E123 (2011).

[22] C. Domain and C. S. Becquart, Phys. Rev. B **65**, 024103 (2001).

[23] D. Nguyen-Manh, A. P. Horsfield, and S. L. Dudarev, Phys. Rev. B **73**, 020101 (2006).

[24] P.-W. Ma, W. C. Liu, C. H. Woo, and S. L. Dudarev, J. Appl. Phys. **101**, 073908 (2007).

[25] P. Van Zwol, P. M. Derlet, H. Van Swygenhoven, and S. L. Dudarev, Surf. Sci. **601**, 3512 (2007).

[26] P.-W. Ma, C. H. Woo, and S. L. Dudarev, Philos. Mag. **89**, 2921 (2009).

[27] M.-C. Marinica, F. Willaime, and J.-P. Crocombette, Phys. Rev. Lett. **108**, 025501 (2012).

[28] S. L. Dudarev, R. Bullough, and P. M. Derlet, Phys. Rev. Lett. **100**, 135503 (2008).

[29] S. P. Fitzgerald and S. L. Dudarev, Proc. R. Soc. London A **464**, 2549 (2008).

[30] F. Körmann, A. Dick, B. Grabowski, T. Hickel, and J. Neugebauer, Phys. Rev. B **85**, 125104 (2012).

[31] A. I. Lichtenstein, M. I. Katsnelson, and G. Kotliar, Phys. Rev. Lett. **87**, 067205 (2001).

[32] Y. Kakehashi, S. Akbar, and N. Kimura, Phys. Rev. B **57**, 8354 (1998); Philos. Mag. **86**, 11 (2006); Adv. Phys. **53**, 497 (2004); Y. Kakehashi and M. A. R. Patoary, J. Phys. Soc. Jpn. **80**, 034706 (2011).

[33] M. Uhl and J. Kübler, Phys. Rev. Lett. **77**, 334 (1996).

[34] B. I. Reser, J. Phys.: Condens. Matter **11**, 4871 (1999); **14**, 1285 (2002); J. Magn. Magn. Mater. **258**, 51 (2003); B. I. Reser and N. B. Melnikov, J. Phys.: Condens. Matter **20**, 285205 (2008); N. B. Melnikov, B. I. Reser, and V. I. Grebennikov, *ibid.* **23**, 276003 (2011).

[35] N. M. Rosengaard and B. Johansson, Phys. Rev. B **55**, 14975 (1997).

[36] S. V. Halilov, H. Eschrig, A. Y. Perlov, and P. M. Oppeneer, Phys. Rev. B **58**, 293 (1998).

[37] P. Fazekas, *Lecture Notes on Electron Correlation and Magnetism* (World Scientific Publishing, Singapore, 1999), Chap. 7.

[38] U. Atxitia, O. Chubykalo-Fesenko, R. W. Chantrell, U. Nowak, and A. Rebei, Phys. Rev. Lett. **102**, 057203 (2009).

[39] T. Bose and S. Trimper, Phys. Rev. B **81**, 104413 (2010); **83**, 134434 (2011).

[40] W. C. Kerr and A. J. Graham, Eur. Phys. J. B **15**, 305 (2000).

[41] R. L. C. Akkermans, in *New Algorithms for Macromolecular Simulation*, edited by B. Leimkuhler (Springer, Berlin, 2005), pp. 155–164.

[42] R. Zwanzig, *Nonequilibrium Statisical Mechanics* (Oxford University Press, New York, 2001).

[43] N. G. Van Kampen, *Stochastic Processes in Physics and Chemistry* (North-Holland, Amsterdam, 1981).

[44] O. Gunnarsson, J. Phys. F **6**, 587 (1976).

[45] D. Nguyen-Mahn and S. L. Dudarev, Phys. Rev. B **80**, 104440 (2009).

[46] P. M. Derlet and S. L. Dudarev, Prog. Mater. Sci. **52**, 299 (2007).

[47] S. L. Dudarev and P. M. Derlet, J. Computer-Aided Mater. Des. **14**, 129 (2007).

[48] M. Y. Lavrentiev, R. Soulairol, C.-C. Fu, D. Nguyen-Manh, and S. L. Dudarev, Phys. Rev. B **84**, 144203 (2011).

[49] A. L. Wysocki, J. K. Glasbrenner, and K. D. Belashchenko, Phys. Rev. B **78**, 184419 (2008).

[50] H. Hasegawa, M. W. Finnis, and D. G. Pettifor, J. Phys. F **15**, 19 (1985).

[51] M. Y. Lavrentiev, S. L. Dudarev, and D. Nguyen-Manh, J. Nucl. Mater. **386–388**, 22 (2009).

[52] S. Shallcross, A. E. Kissavos, V. Meded, and A. V. Ruban, Phys. Rev. B **72**, 104437 (2005).

[53] R. Singer, F. Dietermann, and M. Fähnle, Phys. Rev. Lett. **107**, 017204 (2011).

[54] R. Drautz and D. G. Pettifor, Phys. Rev. B **84**, 214114 (2011).

[55] M. van Schilfgaarde and V. A. Antropov, J. Appl. Phys. **85**, 4827 (1999).

[56] J. P. Perdew, K. Burke, and M. Ernzerhof, Phys. Rev. Lett. **77**, 3865 (1996).

[57] S. Lounis and P. H. Dederichs, Phys. Rev. B **82**, 180404 (2010).

[58] S. Morán, C. Edere, and M. Fähnle, Phys. Rev. B **67**, 012407 (2003).

[59] R. F. Sabiryanov and S. S. Jaswal, Phys. Rev. Lett. **83**, 2062 (1999).

[60] V. L. Moruzzi, P. M. Marcus, K. Schwarz, and P. Mohn, Phys. Rev. B **34**, 1784 (1986).

[61] H. A. Mook, J. W. Lynn, and R. M. Nicklow, Phys. Rev. Lett. **30**, 556 (1973).

[62] J. W. Lynn, Phys. Rev. B **11**, 2624 (1975).

[63] H. A. Mook and J. W. Lynn, J. Appl. Phys. **57**, 3006 (1985).

[64] P. J. Brown, H. Capellmann, J. Déportes, D. Givord, and K. R. A. Ziebeck, J. Magn. Magn. Mater. **30**, 243 (1982).

[65] M. Acet, E. F. Wassermann, K. Andersen, A. Murani, and O. Schärpff, Europhys. Lett. **40**, 93 (1997).

[66] P.-W. Ma, S. L. Dudarev, and C. H. Woo, Phys. Rev. B **85**, 184301 (2012).

[67] E. Carpene, E. Mancini, C. Dallera, M. Brenna, E. Puppin, and S. De Silvestri, Phys. Rev. B **78**, 174422 (2008).

[68] K. Furutsu, J. Res. Natl. Bur. Stand., Sect. D **67**, 303 (1963).

[69] E. A. Novikov, Zh. Eksp. Theor. Fiz **47**, 1919 (1964) [Sov. Phys. JETP **20**, 1290 (1965)].

[70] I. Cook, Plasma Phys. **20**, 349 (1978).

[71] A. Ishimaru, *Wave Propagation and Scattering in Random Media* (Academic, New York, 1978).